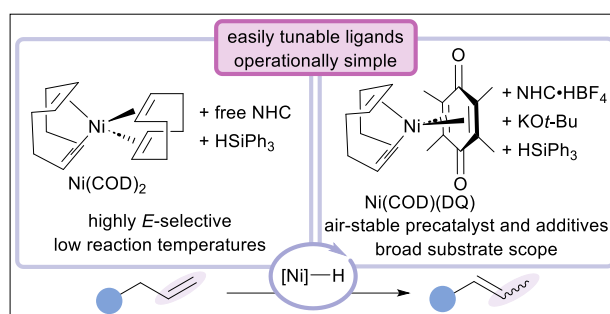


Tuneable, *In Situ*-Generated Nickel-Hydride Alkene Isomerization Catalyst

Melanie A. Kascoutas,^a Alison Sy-min Chang,^a Kiana E. Kawamura,^a Gabriela M. Bailey,^a Parker T. Morris,^a Elizabeth A. Borst,^a Lilliana H. Granados,^a Amanda K. Cook^{*,a}

^aDepartment of Chemistry and Biochemistry, University of Oregon, Eugene, OR 97403, United States

Abstract: A modular, operationally practical Ni(0)/silane alkene isomerization system has been developed with air-stable reagents. A diverse array of functional groups are tolerated, including aryl bromides, aromatic heterocycles, tertiary amines, and α,β -unsaturated amides. Mechanistic experiments support a Ni–H insertion/elimination pathway.



Alkenes are abundant feedstock chemicals frequently used in a variety of synthetic applications like constructing natural products, pharmaceuticals, and commodity chemicals.^{1,2} One efficient route to synthesize internal alkenes is through transition metal-catalysed alkene isomerization (Fig. 1a).² This industrially pertinent process is invoked in important processes such as the DuPont adiponitrile process, which utilizes a homogeneous Ni–H active catalyst (Fig. 1b).¹ Alkene isomerization catalysts composed of 2nd and 3rd row transition-metals have been designed to control specific positional and geometric (*E/Z*) selectivities;³ however, recent focus has shifted to the development of Earth-abundant base metals as more sustainable and economical alternatives to precious-metal catalysts.⁴ While efforts have yielded significant improvements with Fe- and Co- metal catalysts,^{5,6} Ni remains challenging to rationally control and lower catalyst loadings.

Notable advancements in Ni–H alkene isomerization catalysts have been shown by Schoenebeck,⁷ Fleischer,⁸ Ogoshi,⁹ Engle and Vantourout,¹⁰ and Cook^{11,12} which employ mild reaction conditions to achieve high yields and selectivities. However, a common drawback for these catalysts is the requirement of a strict inert atmospheric condition for reaction setup, significantly hindering synthetic practicality. Furthermore, with the exception of work by Ogoshi and Engle and Vantourout, these catalysts lack demonstration of tuneable ancillary ligands to achieve specific catalytic activity. Our group recently developed a modular Ni(0)/silane alkene isomerization catalyst that is sterically tuneable through *N*-heterocyclic carbene (NHC) ancillary ligands and electronically tuneable through 3° silanes; mechanistic experiments point towards a Ni–H active catalyst, which forms through the oxidative addition of a Si–H bond.¹¹ Despite these advances, this system has practical limitations, requiring strict air- and moisture-free conditions

and a multi-step synthetic process to obtain the Ni precatalyst. To overcome these limitations, we hypothesized that the active catalyst could be formed *in situ*, allowing for the use of and rapid evaluation of air-stable, commercially available or easily synthesized, and tuneable catalyst components.

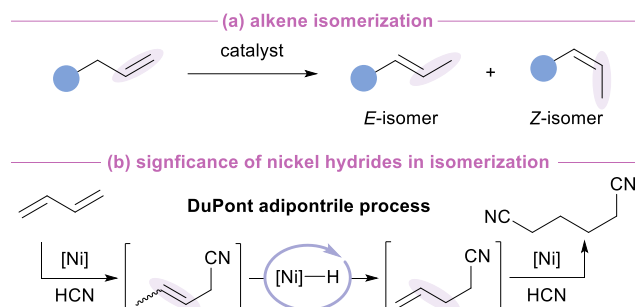


Fig. 1. Background of (a) alkene isomerization, (b) nickel hydrides.

In this study, we report an *in situ*-generated alkene isomerization catalyst using commercially available Ni(0) sources paired with an NHC ligand (the free carbene or the salt + base), and triphenylsilane. Through this approach, we rapidly evaluated a variety of NHCs with varied steric and electronic properties. The optimal NHC was found to be ^{Me}IPr (1,3-bis(2,6-diisopropylphenyl)-4,5-dimethyl-2-imidazolylidene), achieving high product yield and *E*-selectivity. We show that this reaction readily proceeds at near-ambient temperature (30 °C) using ^{Me}IPr/Ni(COD)₂ (COD = 1,5-cyclooctadiene), albeit using the glovebox to set up the reaction to reach maximum efficiency. To circumvent glovebox usage, we developed a moisture-tolerant benchtop system using Ni(COD)(DQ) (DQ = duroquinone), an imidazolium salt, and base that efficiently isomerizes alkenes at moderate reaction temperatures (60 °C). A diverse array of functional groups is tolerated. Preliminary mechanistic experiments including isotopic-labelling experiments and radical-probe studies suggest a Ni–H insertion/elimination pathway is occurring. This Ni(0)/silane catalyst offers increased modularity and synthetic practicality than previous reports, increasing its potential application in organic synthesis.

Inspired by our previous work, in which (IPr)Ni(1,5-hexadiene)/Ar₃SiH (IPr, 1,3-bis[2,6-bis(1-methylethyl)phenyl]-1,3-dihydro-2*H*-imidazol-2-ylidene; Ar, aryl) was the optimal precatalyst, we hypothesized that the same active Ni–H catalyst could be generated *in situ* by reacting Ni(COD)₂, IPr, and triphenylsilane (HSiPh₃). Under analogous reaction conditions (80 °C, toluene), allylbenzene (**1a**) was isomerized to β-methylstyrene (**2a**) in 87% yield and good *E/Z* selectivity of 21:1 (Table 1, entry 1). Lowering the reaction temperature to 60 °C and 40 °C significantly diminished yields (46 and 20%, respectively, Table 1, entries 2-3), indicating that an elevated temperature is required with IPr. Taking advantage of the *in situ* catalyst design, we evaluated a series of NHCs with various steric parameters at 40 °C (Table 1, entries 4-8) to identify the optimal ligand. A set of readily accessible NHCs were evaluated and compared to IPr (Fig. 2). ITMe (1,3,4,5-tetramethylimidazol-2-ylidene), IMes (1,3-bis[2,4,6-trimethylphenyl]-1,3-dihydro-2*H*-imidazol-2-ylidene), and SIPr (1,3-bis[2,6-diisopropylphenyl]-imidazolidine-2-ylidene) all gave lower yields of **2a** (5.0%, 4.2%, and 9.6%; Table 1, entries 4-6, respectively) than IPr. However,

using both ^{Cl}IPr (1,3-bis[2,6-diisopropylphenyl]-4,5-dichloro-1,3-dihydro-2*H*-imidazol-2-ylidene) and ^{Me}IPr resulted in increased yields (24% and 86%; Table 1, entries 7 and 8, respectively) and selectivities (*E/Z* = 43:1 and 35:1, respectively), with ^{Me}IPr being identified as the best ligand in this series. Lowering the reaction temperature to 30 °C using ^{Me}IPr afforded a similar yield of 81% **2a** with further increased *E/Z* selectivity to 63:1 (Table 1, entry 9), favouring the thermodynamically more favoured *E*-isomer.

Table 1. Optimization of the Ni(COD)₂/NHC/Ph₃SiH-catalysed alkene isomerization. Yields and selectivity determined by GC analysis using 1,2,4,5-tetramethylbenzene as an internal standard.

C=CCc1ccccc1 (1a) $\xrightarrow[\text{toluene, 7 h}]{\text{Ni(COD)}_2 \text{ (5 mol \%), IPr (5 mol \%), HSiPh}_3 \text{ (5 mol \%)}} \text{C=CCc1ccccc1} (2a)$

Entry	Deviation from standard conditions	Temp. (°C)	GC yield	Selectivity (<i>E/Z</i>)
1	-	80	87%	21:1
2	-	60	46%	26:1
3	-	40	20%	31:1
4	ITMe	40	5.0%	15:1
5	IMes	40	4.2%	13:1
6	SIPr	40	9.6%	31:1
7	^{Cl} IPr	40	24%	43:1
8	^{Me} IPr	40	86%	35:1
9	^{Me} IPr	30	81%	63:1

After establishing the *in situ* alkene isomerization catalytic system using Ni(COD)₂, we sought to develop a more practical reaction setup that uses air-stable reagents. We exchanged the air-sensitive Ni(COD)₂ for air-stable Ni(COD)(DQ) and the free NHC to an imidazolium salt with a base to form the free carbene in solution.¹³ Testing the isomerization of 4-allylanisole (**1b**) using IPr•HBF₄ and KO*t*-Bu at 60 °C afforded 94% **2b** with good selectivity of 24:1 (*E/Z*) after 6 h (Table 2, entry 1). Notably, the results in Table 2, except for entry 2, were collected using nitrogen-sparged solvent and flushing the reaction vessel with nitrogen gas; however, no reactivity is observed when the reaction is run under ambient air (Table 2, entry 2). These data suggest that water does not impact catalysis, but oxygen does inhibit the desired activity. Control experiments demonstrated the necessity of each reaction component for isomerization, as very little (or no) **2b** is formed upon the exclusion of the Ni source, imidazolium salt, base, or silane (Table 2, entries 3-6). We next investigated the characteristics of the imidazolium salt. Exchanging the BF₄ counter ion with triflate (OTf) yielded similar results (92% yield, *E/Z* = 23:1, Table 2, entry 7). Replacing IPr•HBF₄ with sterically smaller imidazolium salts, ItBu•HBF₄ (1,3-di-*tert*-butylimidazolium tetrafluoroborate) and IMes•HBF₄, resulted in minimal isomerization (Table 2, entries 8-9).¹⁴ However, increasing the steric bulk, as seen in the Ni(COD)₂/NHC system, improved the yield to 97% while maintaining good selectivity (*E/Z* = 25:1) (Table 2, entry 10). We attempted to lower

the reaction temperature from 60 °C to increase *E*-selectivity, however isomerization no longer occurred, which we attribute to low solubility of the precatalyst and additives (Table 2, entry 11).

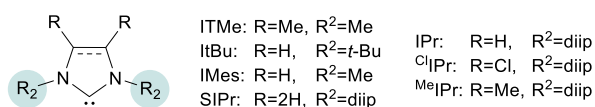


Fig. 2. Library of NHC ligands tested with Ni(0) sources.

Table 2. Reaction optimization using Ni(COD)(DQ), an imidazolium salt, and a base for the isomerization of **1b**. Yields and selectivity determined by GC analysis using cyclooctane as an internal standard. ^an.d., not determined. ^breported at 1 h.

Ni(COD)(DQ) (5 mol %)
 IPr•HBF₄ (5 mol %)
 KO*t*-Bu (10 mol %)
 HSiPh₃ (5 mol %)

Ar = 4-OMe-C₆H₅

$\text{Ar-CH=CH}_2 \xrightarrow[\text{toluene, 60 }^\circ\text{C, 6 h}]{\text{reagents}} \text{Ar-CH=CH-CH}_2$

1b **2b**

Entry	Deviation from standard conditions	GC yield	Selectivity (<i>E/Z</i>)
1	none	94%	24:1
2	Ambient air	0%	n.d. ^a
3	No Ni(COD)(DQ)	0%	n.d.
4	No KO <i>t</i> -Bu	0%	n.d.
5	No HSiPh ₃	8%	74:1
6	No IPr•HBF ₄	0%	n.d.
7	IPr•OTf	92%	23:1
8	ItBu•HBF ₄	0%	n.d.
9	IMes•HBF ₄	11%	32:1
10	MeIPr•HBF ₄	97%	25:1
11	MeIPr•HBF ₄ , 50 °C	0% ^b	n.d.

Because the yield and selectivity of **2b** with IPr•HBF₄ and MeIPr•HBF₄ are similar at 6 h reaction time (Table 2, entries 1 and 10), we sought to differentiate their activity by monitoring the isomerization of **1b** to **2b** over time (ESI Fig. 1). While the reaction completes within 25 min with MeIPr•HBF₄ (ESI Fig. 1, purple circles), completion is not reached within 3 hours using IPr•HBF₄ (ESI Fig. 1, pink squares). Furthermore, IPr•HBF₄ shows a significant induction period (~45 min), while MeIPr•HBF₄ shows a negligible, if any, induction period. Because of the faster initial rate, MeIPr•HBF₄ was chosen as the optimal NHC precursor for isomerization.

Moving forward with optimized conditions, we tested a variety of alkene substrates (Fig. 3). The electron-poor allylbenzene derivative, 4-CF₃-allylbenzene (**1c**) yields 76% product (**2c**) with 33:1 selectivity. The acid-sensitive methoxymethyl ether group was well-tolerated, with product **2d** forming in high reaction yield (97%) with 20:1 selectivity (*E/Z*). 4-Br-allylbenzene (**1e**) affords 53% yield of **2e** with 14:1 selectivity (*E/Z*); this tolerance of an aryl bromide is notable, since Ni complexes are known to react readily with them in oxidative addition reactions.¹⁵ Trisubstituted alkenes are formed in high yields and moderate selectivity, as shown with 2-phenyl-2-pentene (**2f**) (94% yield, *E/Z* = 11:1). Added steric bulk, as seen in 2-methylallylbenzene (**1g**) and allylmesitylene (**1h**), resulted in moderate to good yields but with a decrease in selectivity (*E/Z* = 10:1 and 2.0:1, respectively). Alkene isomerization can be achieved across multiple bonds, as demonstrated with 1-decene (**1i**) and homoallylbenzene (**1j**) to afford a mixture of positional isomers (positional selectivity, p.s. = 1:2.1 and 2.3:1, respectively), and the major isomer of **2j** being 1-buten-1-ylbenzene (*E/Z* = 34:1). The catalyst system tolerates a variety of aromatic heterocycles including pyridine (**1k**), indole (**1l**), thiophene (**1m**), furan (**1n**), affording **2k**, **2l**, **2m**, and **2n**, respectively, in good conversions or yields (84-98%) and moderate to good selectivity (*E/Z* = 4.5-18:1). Notably, this tolerance of heterocycles is a drastic improvement compared to our previously reported (IPr)Ni(1,5-hexadiene) catalyst.¹¹ Other functional groups such as a tertiary amine to form an enamine (**2o**) and a β,γ-unsaturated amide to form an α,β-unsaturated amide (**2p**) are suitable for this reaction, which are also further improvements over previous work. To demonstrate the value and usefulness of this system, a large-scale reaction with **1b** was performed and 1.17 g **2b** (98% yield) was isolated in good selectivity of *E/Z* = 25:1, with the entire reaction set up on the bench with sparging. To exemplify the synthetic utility of enamines generated with our catalyst, a tandem reaction was performed converting allyldiphenylamine (**1o**) to **2o**, and then adding benzaldehyde, resulting in the formation of 2-methyl-3-phenyl-2-propen-1-al (**3a**) in 63% yield.

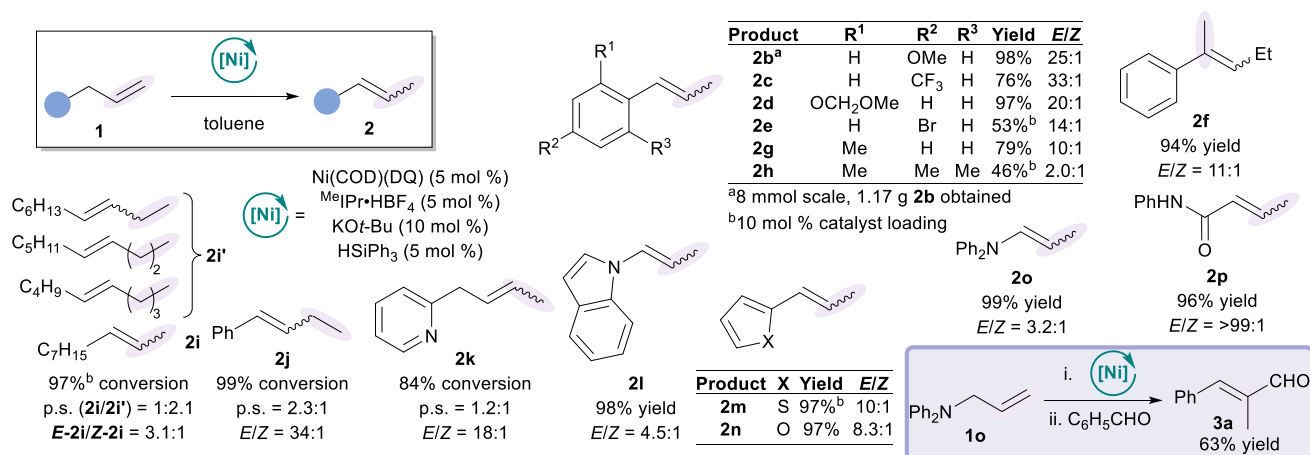


Fig. 3. Substrate scope of alkene isomerization (p.s., positional selectivity).

We next performed mechanistic experiments to extract information on the reaction pathway. We considered three common pathways for Ni-catalysed alkene isomerization including (i) a radical pathway through metal-hydride atom transfer (MHAT), (ii) an intramolecular π-allyl pathway, and (iii) a metal-hydride (M–H) insertion/elimination pathway (Fig. 4a). To differentiate between these possibilities, we designed experiments to unveil the reaction mechanism.

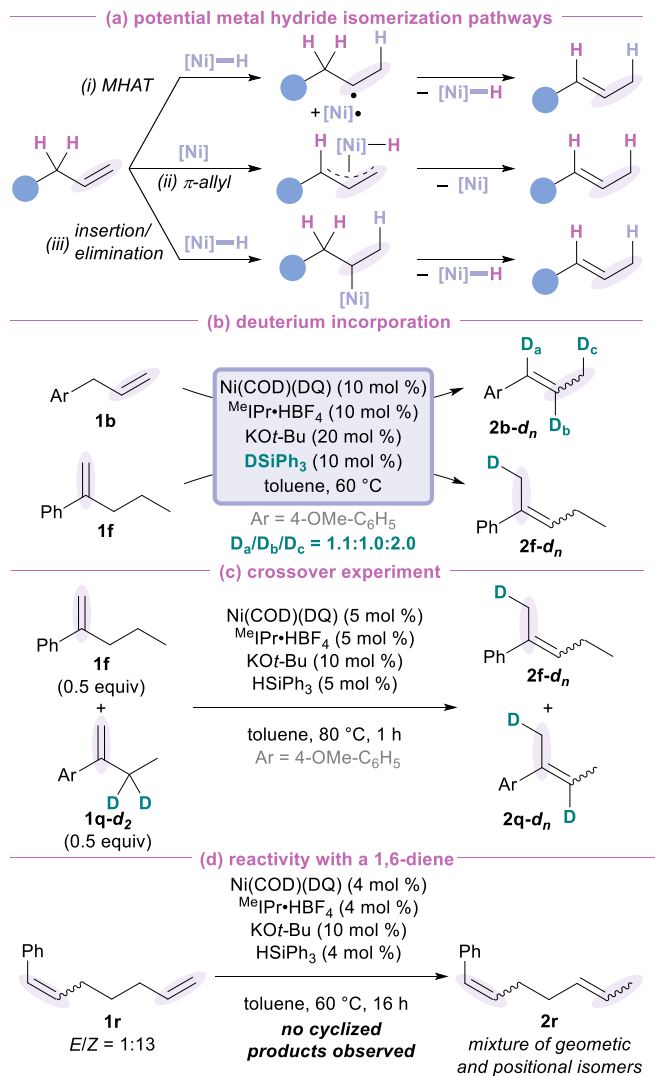


Fig. 4. (a) Potential metal hydride isomerization pathways. (b-d) Various experimental mechanistic studies.

As shown in Table 2, HSiPh₃ is necessary for catalytic activity; we hypothesized that it acts as a hydride source to form the Ni–H active catalyst. Using our standard conditions, the isomerization of **1b** to **2b** was performed using DSiPh₃ to determine if the hydrogen from the silane is incorporated into the product. Deuterium incorporation into the propenyl group is expected for insertion/elimination and MHAT pathways, while no deuterium incorporation is expected for the π-allyl pathway, since the M–H in the π-allyl pathway is formed via C–H activation of an allylic C–H bond. Using substrate **1b**, ²H NMR shows D-incorporation in all three positions along the propenyl chain of **2b**, indicating that isomerization is highly reversible (Fig. 4b, top). To further understand catalyst behaviour, an additional experiment using DSiPh₃ was performed using α-propylstyrene (**1f**) as the substrate. D-incorporation was only observed in the β-methyl group of **2f** (Fig. 4b, bottom). These results signify that Ni–H migratory insertion is reversible for 1,2-disubstituted alkenes, but irreversible for trisubstituted alkenes. This change in reactivity

suggests that trisubstituted alkenes are worse ligands for Ni than 1,2-disubstituted alkenes, and they readily dissociate before β -hydride elimination can occur.¹⁶ Additionally, these D-incorporation studies support our hypothesis that the silane acts as the hydride source and is consistent with the MHAT and insertion/elimination pathways but inconsistent with the π -allyl pathway. A crossover experiment was performed to differentiate between an intra- (π -allyl) and intermolecular (MHAT or Ni–H insertion/elimination) mechanism. A 1:1 mixture of α -propylstyrene (**1f**) and 4'-OMe- α -ethylstyrene- d_2 (**1q-d₂**) were subjected to the standard reaction conditions. If the reaction proceeds through an intramolecular pathway, no deuterium incorporation into **2f** is expected, while if an intermolecular pathway is operative, deuterium incorporation would be expected in **2f**. ²H NMR analysis displays deuterium incorporation into both products **2f** and **2q** (Fig. 4c), which is consistent with the intermolecular pathways, and is inconsistent with the π -allyl pathway.

For our final mechanistic endeavour, we probed the reaction for an MHAT pathway by subjecting a 1,6-diene radical clock (**1r**) under isomerization conditions. If the reaction proceeds through an MHAT pathway, a free radical intermediate will be generated, and **1r** will cyclize into cyclopentane. However, if the reaction proceeds through a two-electron pathway (Ni–H insertion/elimination or π -allyl) no cyclized products are expected to form. Reacting **1r** under standard conditions, only geometric and positional isomerization products were observed, and no cyclized product was detected as determined by ¹H NMR analysis (Fig. 4d). This result suggests that radical species are likely not generated in our catalytic system.

Collectively, these experiments support a Ni–H insertion/elimination mechanism. The Ni–H can be accessed through oxidative insertion of Ni into the R₃Si–H bond; migratory insertion of the coordinated alkene into the Ni–H bond followed by β -hydride elimination to generate the product. Ligand exchange of the isomerized alkene for the starting alkene completes the catalytic cycle.

In conclusion, we have developed a practical alkene isomerization protocol using Ni(0), a silane, and an NHC ancillary ligand. The NHC can be readily modulated to induce desirable catalytic activity. Enabled by the avoidance of the cumbersome and challenging synthesis of (NHC)Ni(0) complexes, ^{Me}IPr was rapidly identified as the best ligand. Under optimized conditions, high yields and *E/Z* selectivities are obtained for a variety of substrates, including allylbenzene derivatives, heterocycles, 1,1-disubstituted alkenes, and enamines. Mechanistic studies suggest the alkene isomerization pathway proceeds through a Ni–H insertion/elimination route. This bench-preparative catalytic system serves as an attractive synthetic method to form internal alkenes from readily abundant terminal alkenes, with facile ligand modularity.

Conflicts of interest

There are no conflicts to declare.

Notes and references

1. C. R. Larsen and D. B. Grotjahn, in *Applied Homogeneous Catalysis with Organometallic Compounds*, John Wiley & Sons, Ltd, 2017, pp. 1365–1378.
2. J. J. Molloy, T. Morack and R. Gilmour, *Angew. Chem. Int. Ed.*, **2019**, 58, 13654–13664.
3. E. Larionov, H. Li and C. Mazet, *Chem. Commun.*, **2014**, 50, 9816–9826.

4. X. Liu, B. Li and Q. Liu, *Synthesis*, **2019**, 51, 1293–1310.
5. X. Yu, H. Zhao, P. Li and M. J. Koh, *J. Am. Chem. Soc.*, **2020**, 142, 18223–18230.
6. S. Zhang, D. Bedi, L. Cheng, D. K. Unruh, G. Li and M. Findlater, *J. Am. Chem. Soc.*, **2020**, 142, 8910–8917.
7. A. Kapat, T. Sperger, S. Guven and F. Schoenebeck, *Science*, **2019**, 363, 391–396.
8. P. M. Kathe, A. Caciuleanu, A. Berkefeld and I. Fleischer, *J. Org. Chem.*, 2020, 85, 15183–15196.
9. H. Iwamoto, T. Tsuruta and S. Ogoshi, *ACS Catal.*, **2021**, 11, 6741–6749.
10. C. Z. Rubel, A. K. Ravn, H. C. Ho, S. Yang, Z.-Q. Li, K. M. Engle and J. C. Vantourout, *Angew. Chem. Int. Ed.*, **2024**, 63, e202320081.
11. K. E. Kawamura, A. S. Chang, D. J. Martin, H. M. Smith, P. T. Morris and A. K. Cook, *Organometallics*, **2022**, 41, 486–496.
12. A. S. Chang, M. Kascoutas, Q. Valentine, K. How, R. Thomas and A. Cook, *J. Am. Chem. Soc.*, **2024**.
13. V. T. Tran, Z.-Q. Li, O. Apolinar, J. Derosa, M. V. Joannou, S. R. Wisniewski, M. D. Eastgate and K. M. Engle, *Angew. Chem. Int. Ed.*, **2020**, 59, 7409–7413.
14. H. Clavier and S. P. Nolan, *Chem. Commun.*, **2010**, 46, 841–861.
15. T. T. Tsou and J. K. Kochi, *J. Am. Chem. Soc.*, **1979**, 101, 6319–6332.
16. C. A. Tolman, *J. Am. Chem. Soc.*, **1974**, 96, 2780–2789.